Acta Polytechnica **65**(2):213–221, 2025
https://doi.org/10.14311/AP.2025.65.0213

Published by the Czech Technical University in Prague

EVALUATION AND MODELLING OF THE BUCKLING BEHAVIOUR OF SRC COMPOSITE COLUMNS UNDER SIMULTANEOUS OFF-AXIS AND LATERAL LOADING

Kabir Sadeghi, Javad Royaei*, Fatemeh Nouban

Near East University, Department of Civil Engineering, Via Mersin 10, Lefkosa, Turkey
* corresponding author: royaei.j1975@yahoo.com

Abstract. In this paper, steel-reinforced composite columns (SRCs) with IPE profiles, commonly used in Iran, have been investigated under lateral and axial loads. The variable parameters in this study are the amount of axial load eccentricity and changes in the ratio of the applied axial load to the lateral load. For this purpose, ABAQUS finite element software has been used. Based on the results, it was observed that as the percentage of eccentricity increased (load to lateral load ratio of 0.5), the buckling load of the composite column has decreased. By increasing the eccentricity from 0 % to 100 %, the buckling load reduction rate for the first mode of the column is equal to 3 % and the amount of critical load reduction in this condition is equal to 21 %. It was also observed that the buckling load of the composite column decreased as the percentage of eccentricity increased (load to lateral load ratio of 1), by increasing the eccentricity from 0 % to 100 %, the buckling load reduction rate for the first mode of the column is equal to 4 % and the amount of critical load reduction in this condition is equal to 20 %.

Keywords: Composite sections, SRC columns, buckling, ABAQUS.

1. Introduction

Today, the use of composite columns has become very popular all over the world. Composite columns are a clever combination of steel and concrete, offering the advantages of both materials at the same time [1]. Composite columns are divided into two categories based on the placement of the steel and concrete: full concrete composite columns or concrete-filled tubes (CFT) and steel-reinforced composite columns (SRC), which are embedded in concrete. SRCs consist of a steel profile in the centre surrounded by reinforced concrete [2–5]. This research investigates the behaviour of composite columns embedded in concrete with IPE profiles, which are commonly used in Iran, under axial loading by leaving different centres and under simultaneous application of lateral and compressive load. The variable parameters in this study are the amount of axial load eccentricity and changes in the ratio of axial load to applied lateral load. For this purpose, ABAQUS finite element software was used. Due to the many features and advantages of composite sections and composite columns and the appropriate seismic behaviour of this type of section, their use in a country with a high seismic activity such as Iran is very important [6]. Therefore, it is necessary to study the behaviour of these types of structural elements to gain a better understanding of their performance. Based on the articles studied in the field of research [7, 8], it has been observed that the effect of eccentricity has been studied for axial load conditions and the effect of the lateral load has not been considered, and the effect of the ratio of axial load to lateral load on the behaviour of this type of member has been less studied.

Liu [9] investigated the seismic behaviour of CFT square sections for beams-columns on a biaxial bending machine. Various experiments have been performed on CFT columns under the combined load of fixed axial load and cyclic lateral load and at different angles to the cross-sectional axis. Pereira et al. [10] investigated the off-plane axial bearing capacity for high-strength steel composite columns with various cross-sectional shapes. Csuka et al. [11] analysed finite FRP columns under off-axis loads. A new model for FRP limited concrete columns is applied to the rectangular sections loaded from the axis and from the centre. Good agreement was found between the calculations, the experimental data and what was found in the literature. Wu et al. [12] investigated the effect of load eccentricity on the FRS-enclosed stress relationship of concrete columns. This paper presents an experimental and analytical study on FRP circular concrete columns under off-axis loading. 36 short concrete cylinders were tested under different loads and FRP jacket stiffness. Based on the analysis of the test results, a new model has been developed for the stress-stress relationship of FRP columns under off-axis loading. It is concluded that the forward-stress models for concentrated loading columns are insufficient to predict the column response for off-axis loading. The stress-strain curve shows a significant stiffening trend when the load is off-centre. Kottb et al. [13] investigated the behaviour of high-strength concrete columns under off-axis loads. The columns analysed with the experimental results showed an average difference of

16 % and 17 % for the final load of the column and the middle height displacement, respectively. The results showed that there was excellent agreement for the crack patterns. Predicting the capacity of the columns using interaction diagrams based on the ACI 318-08 stress block parameters showed that a safe design method of the HSC column in external compression is to reinforce them with ACI 318-08 Carter protection for HSC columns. Qu et al. [14] conducted an experimental study of a rectangular CFST column under eccentric loading. The proportion of concrete required for CFST rectangular columns capable of withstanding anomalous loads was also obtained by comparing the simulated results and the test data. Finally, based on the definitions and conclusions for the design strength of CFST rectangular columns based on the "Technical Specifications for the Design of Steel Houses in Tianjin" (DB 29-57-2003), a β factor to increase the strength of steel to pay attention to the contribution of concrete to the strength, the modified equation can then provide a better understanding and the ability to more accurately predict the value. Sun et al. [15] conducted an experimental study on the behaviour of GFRP reinforced concrete columns under non-central axial load. In addition, the GFRP strain pressure curves on the tensile side on which the GFRP-RCCs were subjected to axial loads were reduced, and the rate of reduction was less than in the compression zone. This study also showed that the bond behaviour between GFRP rods and concrete improves when GFRP rods are used as longitudinal compression rods.

The buckling behaviour of steel-reinforced composite (SRC) columns under combined off-axis axial and lateral loading is complex, involving non-linearities in both geometry and material properties. Given the intricacies introduced by eccentric loading, varying load ratios, and the interaction between the axial and lateral forces, an analytical solution to this type of stability problem is not readily available in closed form. Approximate methods such as the finite element method (FEM) are widely used when analytical solutions are difficult or impossible to derive due to the complexity of the geometry, loading conditions, and boundary conditions involved. In this study, the finite element software ABAQUS is chosen to simulate the buckling behaviour of SRC columns because:

(1.) Non-Linearity Handling: ABAQUS can efficiently handle the non-linear behaviour of materials and structures, which is essential in capturing the true buckling response of composite sections.

(2.) Load Eccentricity and Complex Geometry: The inclusion of eccentric loading and the interaction between lateral and axial loads introduces complex stress distributions that are difficult to address analytically. Finite element methods allow for these complexities to be accounted for accurately.

(3.) Model Validation: Previous studies and experimental data have demonstrated the accuracy of finite element models in predicting buckling loads for similar structural systems. Validation of the model against established literature provides further confidence in the method of choice.

2. Mathematical model used and validation

To determine how varying eccentricities of the axial load and the ratio of axial to lateral loads affect the critical buckling load in different modes of the column, we can consider the SRC column to be subjected to:

- An axial load, denoted by P_a, which is applied with eccentricity e.
- A lateral load, denoted by P_l, applied perpendicular to the axis of the column.

The goal of the study is to find the critical buckling load P_{cr}, for both the first and second buckling modes, as a function of:

(1.) Eccentricity e of the axial load.

(2.) Ratio of axial load P_a to lateral load P_l.

Mathematical Model for Buckling Stability
The stability analysis of the SRC column under combined loading can be described using the following mathematical framework:

(1.) **Differential Equation of Equilibrium:** For a column subjected to axial load P_a and lateral load P_l, the equilibrium condition is derived from Euler's buckling theory, considering the effects of eccentricity. The governing differential equation, Equation (1), for the lateral displacement $v(x)$ along the length L of the column is:

$$EI\frac{d^4v(x)}{dx^4} + P_a\left(\frac{d^2v(x)}{dx^2}\right) + P_l v\,(x) = P_a e, \quad (1)$$

where

EI is the flexural rigidity of the column (modulus of elasticity E times moment of inertia I),

P_a is the axial load,

P_l is the lateral load,

$v(x)$ is the lateral displacement as a function of position x along the column's length.

(2.) **Boundary Conditions:** The column may have various boundary conditions depending on its supports:

- Pinned-Pinned:
  $v(0) = v(L) = 0,\ \frac{d^2v(0)}{dx^2} = \frac{d^2v(L)}{dx^2} = 0.$
- Fixed-Free (Cantilever):
  $v(0) = \frac{dv(0)}{dx} = 0,\ \frac{d^2v(0)}{dx^2} = \frac{d^2v(L)}{dx^2} = 0.$

These conditions depend on the structural configuration assumed in the finite element model.

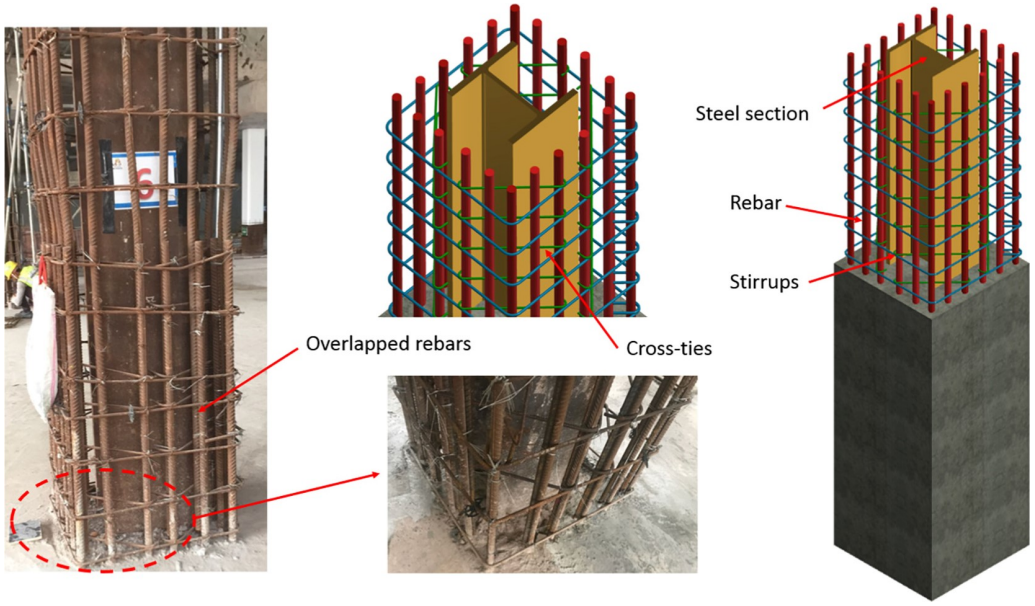

FIGURE 1. Study column [8].

(3.) **Load Eccentricity Consideration:** The axial load P_a applied with eccentricity e introduces an additional moment:

$$M = P_a e. \tag{2}$$

This modifies the lateral displacement equation by introducing a bending moment that depends on the eccentricity. The equation then transforms to Equation (1).

Buckling Criterion: The critical buckling load P_{cr} can be determined by solving the above differential equation for the condition where non-trivial lateral displacements $v(x)$ arise. The critical load is the smallest value of P_a at which the equilibrium solution becomes unstable. For a given mode, the buckling load is given by:

$$P_{cr} = \frac{\pi^2 EI}{(KL)^2}, \tag{3}$$

where K is the effective length factor depending on the boundary conditions and L is the length of the column.

(4.) **Effect of Lateral Load and Eccentricity:** The combined effect of lateral load and eccentricity on the buckling behaviour is accounted for by varying P_l and e in the model and recalculating P_{cr}. The results demonstrate that increasing eccentricity and lateral load leads to a reduction in the buckling load for both buckling modes.

The results of Lai et al. [8] were used for review and validation. In this paper, an SRC column is investigated under buckling analysis. The following Figures 1 and 2 provide an overview of the model.

The CES1 model has been modelled, the specifications of which are as follows. Material properties of the validation model are presented in Table 1. The

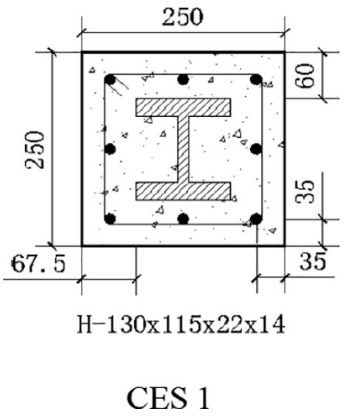

FIGURE 2. Geometric specifications of the validation model [8].

results of the buckling analysis for the columns are shown in Figure 3. In Figure 4, the final model built in the ABAQUS software is presented. The output of the two models is compared and the results are presented in Figure 5.

Based on the comparison of the results obtained from the validation and modelling in ABAQUS software, it has been observed that the difference in results is about 2.3 %. Both models exhibit a similar load-deflection trend, with minor discrepancies in the mid-range deflection (2–6 mm) where the ABAQUS model predicts slightly lower loads. However, the maximum load capacity is consistent, indicating a reliable validation of the numerical model against the reference data.

The objective of this study is to evaluate the buckling behaviour of steel-reinforced composite (SRC) columns under varying eccentricities and different ratios of axial to lateral loads. To achieve this, a systematic experimental planning approach was employed.

Specimen	CES1	
Geometric properties	Section size [mm × mm]	250 × 250
	Steel profile [height × width × web thickness × flange thickness mm]	130 × 115 × 14 × 22
	Length L_0/L [mm]	2 800/3 305
	Slenderness ratio	13.22
	Link spacing	100
	Steel area ratio	10.02 %
	Reinforcement ratio	1.92 %
Material properties	f'_c [MPa]	96
	f_{ss} [MPa]	380
	f_{sl} [MPa]	520
	f_{st} [MPa]	340
	E_{ss} [GPa]	212
	E_{sl} [GPa]	185
	E_{st} [GPa]	201

Table 1. Material properties of the validation model [8].

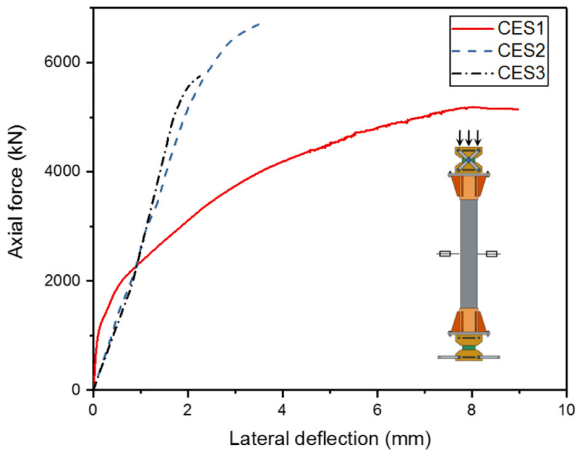

Figure 3. Results of buckling analysis for the columns [8].

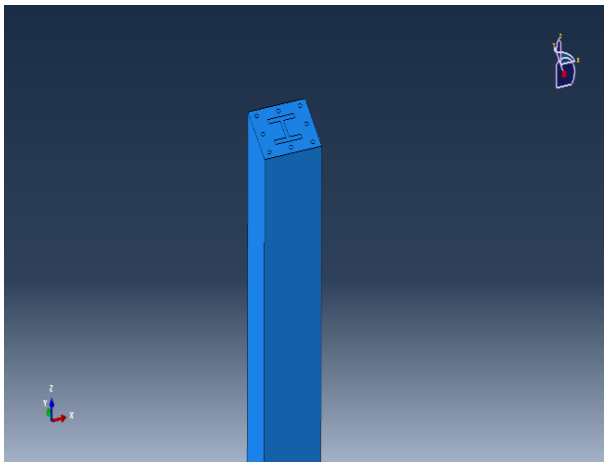

Figure 4. Modelled column.

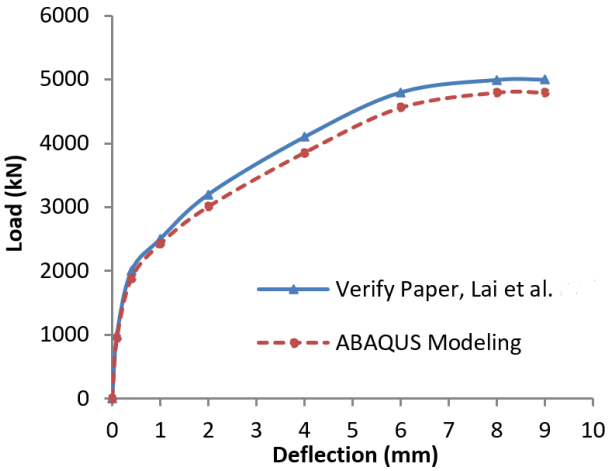

Figure 5. Comparison of results.

(1.) **Parameter Selection:** The key variable parameters considered in the study are:

- Eccentricity (e): The offset of the axial load from the centreline, ranging from 0 % to 100 %.
- Load Ratio $\left(\frac{P_a}{P_l}\right)$: The ratio of axial load to lateral load, with two specific values (0.5 and 1) representing different loading conditions.

(2.) **Experimental Design Approach:** The authors adopted a full factorial design approach, which ensures that all combinations of the selected parameters (eccentricity and load ratio) are investigated. This approach allows for the exploration of interactions between variables and provides a comprehensive understanding of how these factors influence the buckling behaviour of the columns.

- Factor Levels: Eccentricity was varied in 20 % increments, resulting in six levels (0 %, 20 %, 40 %, 60 %, 80 %, and 100 %). For each eccentricity level, two load ratios were investigated (0.5 and 1).

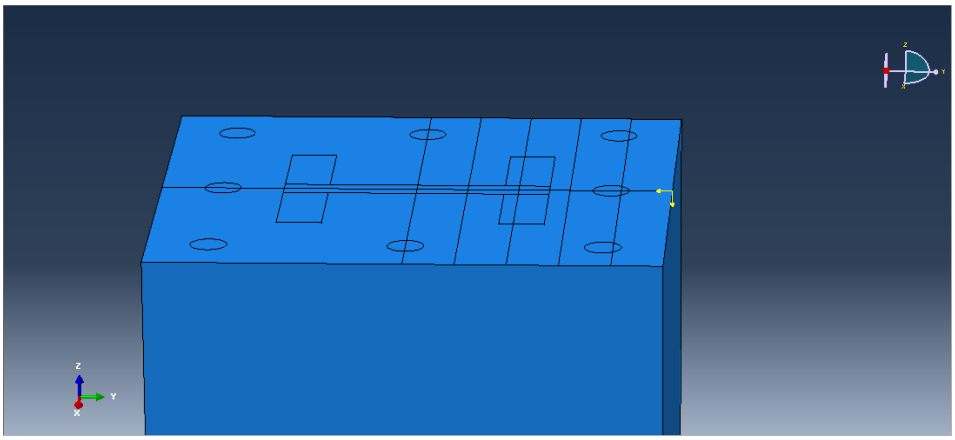

FIGURE 6. Load application position in 100 % eccentricity model with a compressive load to lateral load ratio 0.5.

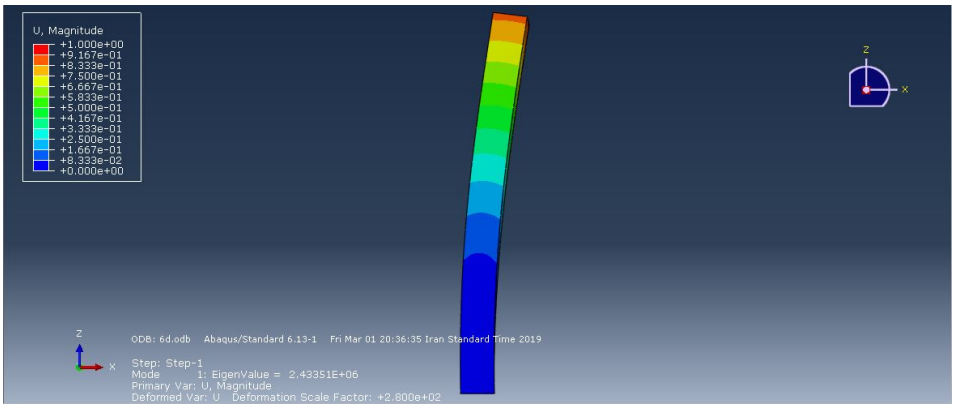

FIGURE 7. The first buckling mode of the 100 % eccentricity model with a compressive load to lateral load ratio of 0.5.

- Simulation Runs: This design resulted in a total of 12 simulation runs (6 eccentricity levels × 2 load ratios). Each run was conducted using the ABAQUS finite element software to simulate the buckling behaviour of the SRC columns.

(3.) **Replication and Verification:** To ensure the reliability of the results, each simulation was replicated twice. Additionally, a mesh sensitivity analysis was conducted to verify that the mesh density did not significantly affect the results.

(4.) **Response Variables:** The response variables of interest were:

- First mode buckling load (P_{cr1}).
- Second mode buckling load (P_{cr2}).

These values were recorded for each simulation run and analysed to determine the impact of eccentricity and load ratio on the column's buckling performance.

3. Results and findings

3.1. Eccentricity value variants with a compressive load to lateral load ratio of 0.5

The modelling performed for this section included varying eccentricity with a constant compressive load to lateral load ratio of 0.5. Therefore, the following 6 modes have been modelled and the results of the first and second buckling modes for each mode have been presented:

- 0 % eccentricity,
- 20 % eccentricity,
- 40 % eccentricity,
- 60 % eccentricity,
- 80 % eccentricity,
- 100 % eccentricity.

3.2. 100 % eccentricity with a compressive load to lateral load ratio of 0.5

Figure 6 shows the position of the load in the model. The rate of eccentricity in this case is equal to 100 %. Figure 7 shows the first two buckling modes of the column. Based on the modelling results, the value of buckling load in the first mode of this model is equal to 243.3 tons. Based on the modelling results shown in Figure 8, the value of buckling load in the second mode of this model is equal to 295.7 tons.

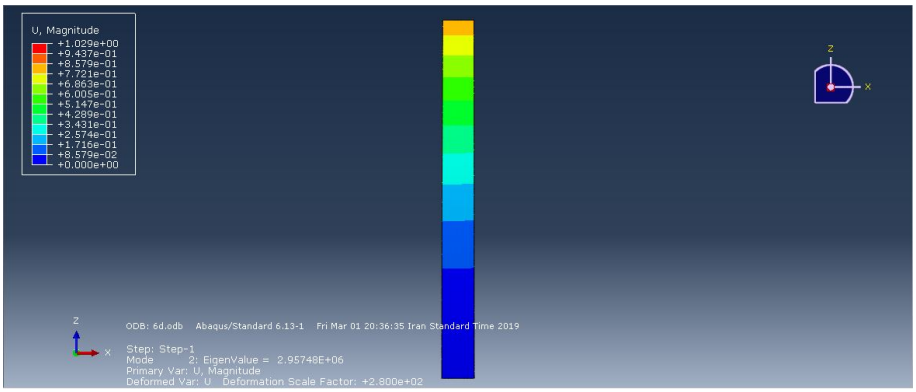

Figure 8. Second buckling mode of 100 % eccentricity model with a compressive load to lateral load ratio of 0.5.

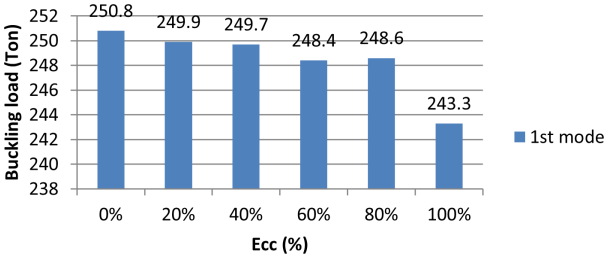

Figure 9. Critical buckling load against the percentage of eccentricity for the first buckling mode with a compressive load to lateral load ratio of 0.5.

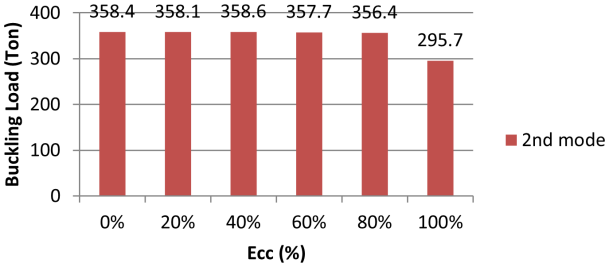

Figure 10. Critical buckling load against the percentage of eccentricity for the second buckling mode with a compressive load to lateral load ratio of 0.5.

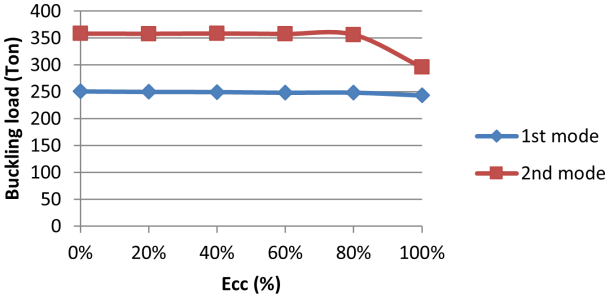

Figure 11. Comparison of the trend of changes in critical buckling load against the percentage of eccentricity for different buckling modes with a compressive load to lateral load ratio of 0.5.

3.3. Summarising the results for varying eccentricity with a constant compressive load to lateral load ratio of 0.5

Figure 9 shows a summary of the eccentricity variants for a ratio of compressive load to lateral load of 0.5. Figure 9 shows the diagram of changes in the critical buckling load against the percentage of eccentricity for the first buckling mode with a compressive load to lateral load ratio of 0.5, the most critical conditions for the buckling load in the first mode are at the load application position at the side edge of the SRC column. 100 % centrality) has occurred. In addition, the best performance for eccentricity of 0 % has been observed.

Figure 10 shows the diagram of changes in the buckling critical load against the percentage of eccentricity for the second buckling mode with a compressive load to lateral load ratio of 0.5, the most critical conditions for the buckling load in the second mode are at the load position at the side edge of the column. 100 %). In addition, the best performance for 40 % eccentricity has been observed.

According to the comparison chart in Figure 11, the trend of changes of the critical buckling load against the percentage of eccentricity in different buckling modes with a compressive load to lateral load ratio of 0.5 has been observed that with increasing the percentage of eccentricity, the buckling load of the composite column decreases. The decrease is gradual, as by increasing the eccentricity from 0 % to 100 %, the buckling load for the first mode of the column decreases from 24.8 tons to 243.3 tons, which is a decrease of 3 %. The decrease in critical load for the second buckling mode in this case was from 358.4 tons to 295.7 tons, which equals to a decrease of 21 %.

3.4. Eccentricity value variants with a compressive load to lateral load ratio of 1

The modelling performed for this section included varying eccentricity with a constant compressive load to lateral load ratio of 1. Therefore, the following 6 modes were modelled and the results of the first and second buckling modes for each mode are presented:

- 0 % eccentricity,
- 20 % eccentricity,

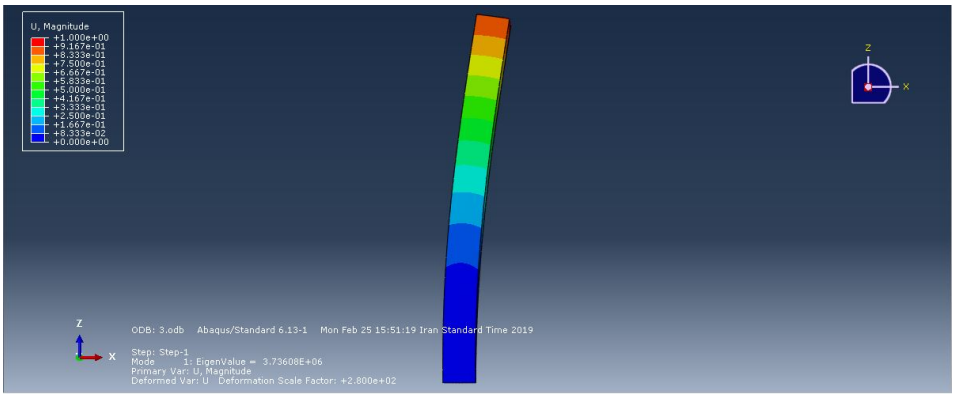

FIGURE 12. First buckling mode of the model with eccentricity of 40 % and a compressive load to lateral load ratio of 1.

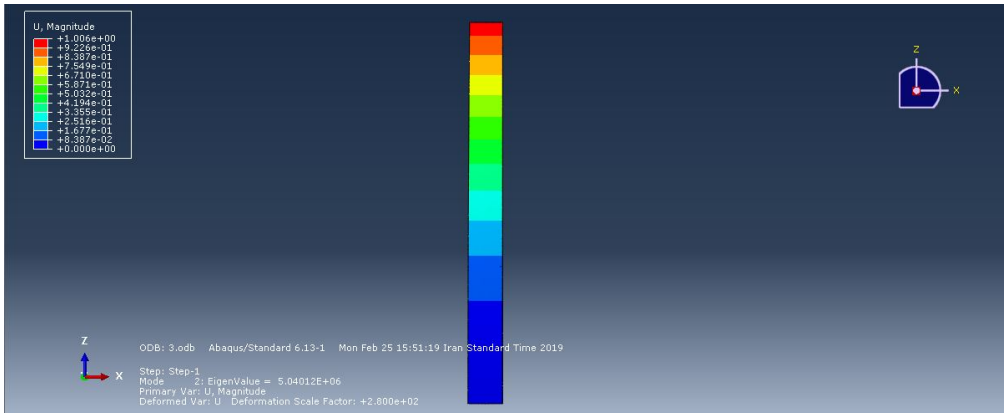

FIGURE 13. Second buckling mode of the model with eccentricity of 40 % and a compressive load to lateral load ratio of 1.

- 40 % eccentricity,
- 60 % eccentricity,
- 80 % eccentricity,
- 100 % eccentricity.

3.5. 40 % ECCENTRICITY WITH A COMPRESSIVE LOAD TO LATERAL LOAD RATIO OF 1

In this case, eccentricity is equal to 40 %. The first two buckling modes of the column are shown below:

From Figure 12, based on the modelling results, it can be clearly seen that the buckling load in the first mode of this model is equal to 373.6 tons.

From Figure 13, based on the modelling results, it can be clearly seen that the buckling load in the second mode of this model is equal to 504 tons.

3.6. SUMMARISING THE RESULTS FOR VARYING ECCENTRICITY WITH A CONSTANT RATIO OF COMPRESSIVE LOAD TO LATERAL LOAD OF 1

Figure 14 shows a summary of the eccentricity variants for a compressive load to lateral load ratio of 1. From Figure 14, based on the diagram of changes in the critical buckling load against the percentage of eccentricity in the first buckling mode with a ratio of

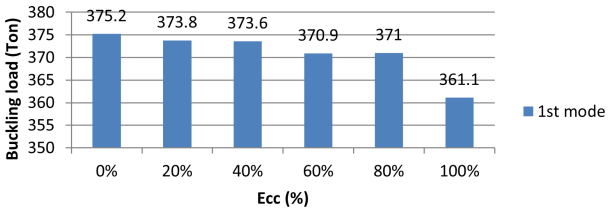

FIGURE 14. Critical buckling load against the percentage of eccentricity for the first buckling mode with a compressive load to lateral load ratio of 1.

compressive load to lateral load of 1, it was observed that the most critical conditions for buckling load in the first mode occurred at 100 % eccentricity. In addition, the best performance was observed at 0 % eccentricity.

From Figure 15, based on the diagram of changes in the critical buckling load against the percentage of eccentricity in the second buckling mode with a compression load to lateral load ratio of 1, it has been observed that the most critical conditions for buckling load in the second mode occurred at 100 % eccentricity. In addition, the best performance has been observed for 40 % eccentricity.

From Figure 16, based on the comparison diagram of the trend of changes in the critical buckling load

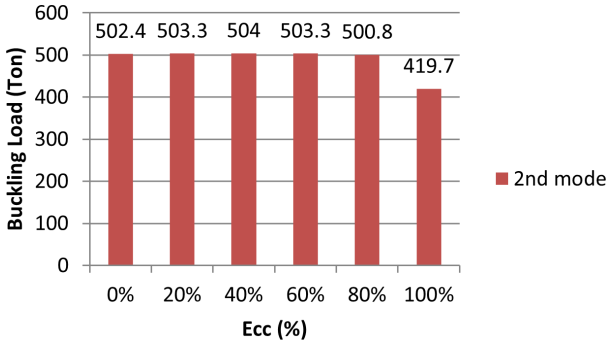

Figure 15. Critical buckling load against the percentage of eccentricity for the second buckling mode with a ratio of compressive load to lateral load of 1.

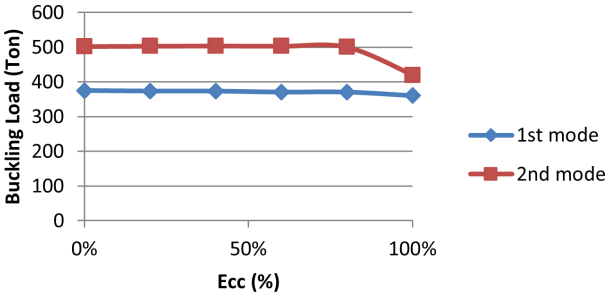

Figure 16. Comparison of the trend of changes in critical buckling load against the eccentricity percentage for different buckling modes with a compressive load to lateral load ratio of 1.

against the percentage of eccentricity in different buckling modes with a compression load to lateral load ratio of 1, it has been observed that as the percentage of eccentricity increases, the buckling load of the composite column has decreases. In the first buckling mode, as the eccentricity increases from 0 % to 100 %, the critical load of the column decreases from 375.2 tons to 361.1 tons, which is a decrease of 4 %. In the case of the second buckling mode, as the eccentricity increases from 0 % to 100 %, the critical load of the column decreases from 502.4 tons to 419.7 tons, which is a decrease of 20 %.

4. Discussion

A numerical analysis was carried out using the ABAQUS finite element software and buckling loads for the first and second buckling modes were obtained for different eccentricities and ratios of compressive to lateral loads.

Table 2 presents the numerical values for the buckling loads for various eccentricities and two buckling modes. The results show that increasing the eccentricity leads to a reduction in the buckling load, especially in the second mode.

The error for the first and second buckling modes for various eccentricities is presented in Table 3.

The error values indicate a good agreement between the simulation results and experimental data, with errors ranging between 2 % and 3.3 % for different buckling modes.

Based on the results of the variation of the critical buckling load against the percentage of eccentricity in the first buckling mode with a compressive load to lateral load ratio of 0.5, it was observed that the most critical conditions for buckling occur at 100 % eccentricity at the side edge of the SRC column. The best performance is observed at 0 % eccentricity. Similarly, for the second buckling mode with a compressive load to lateral load ratio of 0.5, the critical conditions are at 100 % eccentricity, with optimum performance at 40 % eccentricity. The trend in critical buckling load shows a gradual decrease with increasing eccentricity. From 0 % to 100 %, the buckling load decreases by 3 % in the first mode (from 24.8 tons to 243.3 tons) and by 21 % in the second mode (from 358.4 tons to 295.7 tons). For a compressive to lateral load ratio of 1, the first mode shows critical conditions at 100 % eccentricity and best performance at 0 %, while the second mode shows the most critical conditions at 100 % and the best performance at 40 %. The critical buckling load decreases by 4 % in the first mode (from 375.2 tons to 361.1 tons) and by 20 % in the second mode (from 502.4 tons to 419.7 tons) as eccentricity increases from 0 % to 100 %. Doubling the lateral load further decreases the buckling load, reducing it from 375.2 tons to 250.8 tons, a reduction of 49 %.

5. Conclusion

The aim of the research was to investigate the buckling behaviour of steel-reinforced composite (SRC) columns under varying eccentricities and different axial to lateral load ratios. Through a series of finite element simulations, key insights into the effects of eccentricity on buckling performance were obtained. The results provide a valuable understanding for the design of SRC columns, particularly under conditions involving combined loading scenarios. The main findings are summarised below:

- The most critical buckling load conditions in the first mode occur at the side edge of the SRC column at 100 % eccentricity. The best performance is achieved at 0 % eccentricity.
- In the second mode, the most critical buckling load conditions are observed at 100 % eccentricity, while the best performance occurs at 40 % eccentricity.
- An increase in eccentricity from 0 % to 100 % results in a 3 % reduction in buckling load for the first mode, and a 21 % reduction for the second mode.
- The most critical buckling load of the first mode consistently occurs at 100 % eccentricity, while the optimum performance is achieved at 0 % eccentricity.
- The second mode shows the most critical conditions at 100 % eccentricity, with the best performance at 40 % eccentricity.

Eccentricity [%]	Load ratio $[\frac{P_a}{P_l}]$	First mode buckling load [tons]	Second mode buckling load [tons]
0	0.5	375.2	502.4
20	0.5	365.1	490.7
40	0.5	356.8	473.5
60	0.5	348.4	454.8
80	0.5	339.1	434.6
100	0.5	330.4	419.7

TABLE 2. Numerical Results for Buckling Loads (in tons).

Eccentricity [%]	First mode error [%]	Second mode error [%]
0	2.1	2.5
20	2.3	2.7
40	2.0	2.4
60	2.5	2.8
80	2.4	3.1
100	2.6	3.3

TABLE 3. Relative error [%] for first and second buckling modes.

- A 20 % reduction in the critical load of the second mode is observed as the eccentricity increases from 0 % to 100 %.
- Doubling the lateral load leads to a substantial 49 % reduction in buckling load, highlighting the significant impact of increased lateral forces.

REFERENCES

[1] K. A. Skalomenos, G. D. Hatzigeorgiou, D. E. Beskos. Parameter identification of three hysteretic models for the simulation of the response of CFT columns to cyclic loading. *Engineering Structures* **61**:44–60, 2014. https://doi.org/10.1016/j.engstruct.2014.01.006

[2] B. C. Gourley, C. Tort, J. F. Hajjar, P. H. Schiller. A synopsis of studies of the monotonic and cyclic behavior of concrete-filled steel tube beam-columns. Structural Engineering Report ST-01-4, University of Minnesota, Department of Civil Engineering, USA, 2001.

[3] British Standards Institute. BS 5400-2:2006. Steel, concrete and composite bridges: Specification for loads, 2006.

[4] European Convention for Constructional Steelwork. ECCS manual on design of steel structures in seismic zones, 2006.

[5] B. Evirgen, A. Tuncan, K. Taskin. Structural behavior of concrete filled steel tubular sections (CFT/CFSt) under axial compression. *Thin-Walled Structures* **80**:46–56, 2014. https://doi.org/10.1016/j.tws.2014.02.022

[6] J. F. Zhang. *Design of composite columns*. Master's thesis, Helsinki University of Technology Steel Structures Spring, 2004.

[7] M. Johansson, K. Gylltoft. Structural behavior of slender circular steel-concrete composite columns under various means of load application. *Steel and Composite Structures* **1**(4):393–410, 2001. https://doi.org/10.12989/scs.2001.1.4.393

[8] B. Lai, J. Y. R. Liew, A. L. Hoang, M. Xiong. A unified approach to evaluate axial force-moment interaction curves of concrete encased steel composite columns. *Engineering Structures* **201**:109841, 2019. https://doi.org/10.1016/j.engstruct.2019.109841

[9] J. Liu, X. Zhou, S. Zhang. Seismic behaviour of square CFT beam – columns under biaxial bending moment. *Journal of Constructional Steel Research* **64**(12):1473–1482, 2008. https://doi.org/10.1016/j.jcsr.2008.01.013

[10] M. F. Pereira, A. T. Beck, A. L. H. C. El Debs. Reliability of partially encased steel-concrete composite columns under eccentric loading. *Revista IBRACON de Estruturas e Materiais* **10**(2):298–316, 2017. https://doi.org/10.1590/S1983-41952017000200003

[11] B. Csuka, L. P. Kollár. Analysis of FRP confined columns under eccentric loading. *Composite Structures* **94**(3):1106–1116, 2012. https://doi.org/10.1016/j.compstruct.2011.10.012

[12] Y.-F. Wu, C. Jiang. Effect of load eccentricity on the stress-strain relationship of FRP-confined concrete columns. *Composite Structures* **98**:228–241, 2013. https://doi.org/10.1016/j.compstruct.2012.11.023

[13] H. A. Kottb, N. F. El-Shafey, A. A. Torkey. Behavior of high strength concrete columns under eccentric loads. *HBRC Journal* **11**(1):22–34, 2015. https://doi.org/10.1016/j.hbrcj.2014.02.006

[14] X. Qu, Z. Chen, G. Sun. Experimental study of rectangular CFST columns subjected to eccentric loading. *Thin-Walled Structures* **64**:83–93, 2013. https://doi.org/10.1016/j.tws.2012.12.006

[15] L. Sun, M. Wei, N. Zhang. Experimental study on the behavior of GFRP reinforced concrete columns under eccentric axial load. *Construction and Building Materials* **152**:214–225, 2017. https://doi.org/10.1016/j.conbuildmat.2017.06.159